

FlexRender: A Distributed Rendering Architecture for Ray Tracing Huge Scenes on Commodity Hardware

Bob Somers and Zoë J. Wood

California Polytechnic University, San Luis Obispo, CA, U.S.A.

Keywords: Rendering, Distributed Rendering, Cluster Computing.

Abstract: As the quest for more realistic computer graphics marches steadily on, the demand for rich and detailed imagery is greater than ever. However, the current “sweet spot” in terms of price, power consumption, and performance is in commodity hardware. If we desire to render scenes with tens or hundreds of millions of polygons as cheaply as possible, we need a way of doing so that maximizes the use of the commodity hardware that we already have at our disposal. We propose a distributed rendering architecture based on message-passing that is designed to partition scene geometry across a cluster of commodity machines, allowing the entire scene to remain in-core and enabling parallel construction of hierarchical spatial acceleration structures. The design uses feed-forward, asynchronous messages to allow distributed traversal of acceleration structures and evaluation of shaders without maintaining any suspended shader execution state. We also provide a simple method for throttling work generation to keep message queuing overhead small. The results of our implementation show roughly an order of magnitude speedup in rendering time compared to image plane decomposition, while keeping memory overhead for message queuing around 1%.

1 INTRODUCTION

Rendering has advanced at an incredible pace in recent years. At the heart of rendering is describing the world we wish to draw, which has traditionally been done by defining surfaces. While exciting developments in volume rendering techniques happen on a regular basis, it is unlikely we will abandon surface rendering any time soon. The champion of surface representations in rendering, has been the polygonal mesh. Even when used to store smooth surfaces in a compressed way (as with subdivision surfaces), they are usually tessellated into large numbers of fine polygons for rendering. Since their representation is defined explicitly, meshes with fine levels of detail have significantly higher storage requirements. Thus, as the demand for higher visual fidelity increases, the natural tendency is to increase geometric complexity.

Graphics, and ray tracing in particular, has long been said to be a problem that is *embarrassingly parallel*, given that many graphics algorithms operate on pixels independently. Graphics processing units (GPUs) have exploited this fact for years to achieve amazing throughput of graphics primitives in real-time. While processor architectures have become exceedingly parallel and posted impressive speedups,

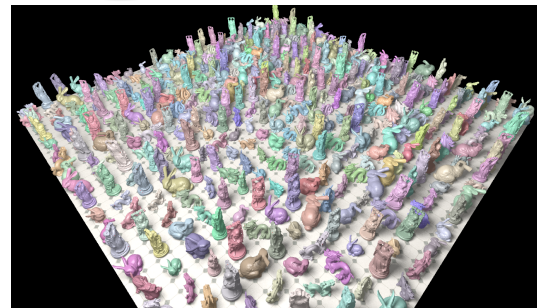


Figure 1: Field of high resolution meshes whose geometric complexity is nearly 87 million triangles. Rendered across 4 commodity machines using FlexRender.

the memory hierarchy has not had time to catch up. For a processor to perform well, the CPI, *cycles per instruction*, must remain low to ensure time is spent doing useful work and not waiting on data.

In current memory hierarchies, data access time can take anywhere from around 12 cycles (4 nanoseconds for an L1 cache hit) to over 300 cycles (100 nanoseconds for main memory). Techniques such as out-of-order execution are helpful in filling this wasted time, but for memory intensive applications it can be difficult to fill all the gaps with useful work.

Because of this fact, there is a lot more to paral-

lel rendering than initially meets the eye. Graphics may indeed be highly parallel, but its voracious appetite for memory access is actively working *against* its parallel efficiency on current architectures.

This paper presents FlexRender, a ray tracer designed for rendering scenes with high geometric complexity on commodity hardware. We specifically target commodity hardware because it currently has an excellent cost to performance ratio, but still typically lacks enough memory to fit large scenes entirely in RAM.

Our work describes the following core contributions:

1. A feed-forward messaging design between workers that passes enough state with every ray to never require reply messages.
2. An approach to shading using this messaging design that does not require suspending execution of shaders and maintaining suspended state.
3. An extension to a stackless BVH traversal algorithm (Hapala et al., 2011) that makes it possible to suspend traversal at one worker and resume it at another.
4. A simple throttling method for managing memory overhead for message queuing without resorting to a complicated dynamic scheduling algorithm.
5. Technical insight into the challenges of building such a renderer, an analysis of our results, and an open-source implementation.

In particular, we show that FlexRender can achieve speedups that are around an order of magnitude better than image plane decomposition for commodity machines, and can naturally self-regulate the cluster of workers to keep the memory overhead due to message queuing around 1% of each worker's main memory.

It is important to remember that FlexRender is an experimental design, and some of our design goals worked better than others. In the hopes of making future experimentation easier for others, we provide the complete source code of FlexRender at <http://www.flexrender.org>.

2 BACKGROUND

FlexRender leverages observations from several fundamental building blocks, including Radiometry, bounding volume hierarchies, and Morton coding.

Radiometry. For the purposes of FlexRender, we note the following observations of the radiometry model of light:

Light Behaves Linearly. The combined effect of two rays of light in a scene is the same as the sum of their independent effects on the scene.

Energy is Conserved. When a ray reflects off of a surface, it can never do so with more energy than it started with.

FlexRender exploits these observations in the following ways:

The Location of Computation does not Matter. If the scene is distributed across many machines, it makes no difference which machine computes the effect of a ray. The sum of all computations will be the same as if all the work was performed on a single machine.

Transmittance Models Energy Conservation. If we store the amount of energy traveling along a ray (the *transmittance*) with the ray itself, we need not know anything about the preceding rays or state that brought this ray into existence. We can compute its contribution to the scene independently and ensure that linearity and energy conservation are both respected.

Bounding Volume Hierarchies. The traversal algorithm of a BVH is naturally recursive, but recursive implementations keep their state on the call stack. In FlexRender, BVH traversal may need to be suspended on one machine and resumed on another, so all of the traversal state needs to be explicitly exposed. Refactoring it as an iterative traversal explicitly exposes the state for capturing, but unfortunately it still requires a traversal stack of child nodes that must be visited on the way back up the tree. In FlexRender, rays carry all necessary state along with them, and this approach would require the entire stack to be included as ray state.

However, (Hapala et al., 2011) presents a stackless traversal method. The key insight is that if parent links are stored in the tree, the same traversal can be achieved using a three-state automaton describing the direction you came from when you reached the current node (i.e. from the *parent*, from the *sibling*, or from the *child*). They show that their traversal algorithm produces identical tree walks and never retests nodes that have already been tested.

FlexRender leverages this traversal algorithm due to its low state storage requirements. Each ray only needs to know the index of the current node it is traversing and the state of the traversal automaton.

Morton Coding and the Z-Order Curve. Morton coding is a method for mapping coordinates in multidimensional space to a single dimension. In particular, walking the multidimensional space with a Morton coding produces a space-filling Z-order curve.

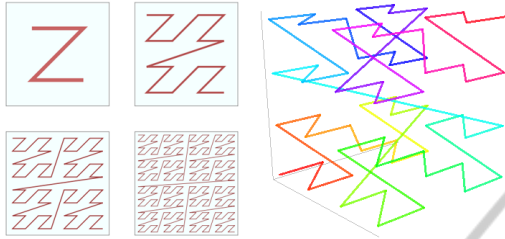


Figure 2: Examples of two dimensional and three dimensional Z-order curves. Credit: “David Eppstein” and “Robert Dickau” (Creative Commons License).

More concretely, FlexRender needs to distribute scene data to machines in the cluster, without a preprocessing step, in a spatially coherent way. If the geometry on each machine consists of a localized patch of the overall geometry, it allows us to minimize communication between the machines, and thus, only pay the network cost when absolutely needed.

Because the Morton coding produces a spatially coherent traversal of 3D space, dividing up the 1D Morton code address space among all the machines participating in the render gives a reasonable assurance of spatial locality for the geometry sent to each machine.

The Morton coding is also simple to implement. For example, to map a point P in a region of 3D space (defined by its bounding extents min and max) to a Morton-coded 64-bit integer, discretizing each axis evenly allows for 21 bits per axis, yielding a 63-bit address space (and one unused bit in the integer). We compute the Morton code by calculating the 21-bit discretized component of P along each axis, then shifting the components from each axis into the 64-bit integer one bit at a time from the most-significant to least-significant bit.

3 RELATED WORK

A number of algorithms are designed to completely avoid large amounts of geometry altogether. Displacement maps (Krishnamurthy and Levoy, 1996) and normal maps using texture data (Cohen et al., 1998) and (Cignoni et al., 1998) are commonly used, especially in real-time applications. However, normal mapping displays visual artifacts, particularly around the edges of the mesh or in areas where the tex-

ture is stretched or compressed. Similarly, level of detail is commonly used to replace high resolution meshes with lower resolution versions when they are far enough away from the viewer (Clark, 1976). However, it requires the creation of multiple resolution meshes and algorithms to smoothly handle resolution changes.

More recently, (Djeu et al., 2011) provides a framework for efficiently tracing multiresolution geometry, but it has large memory requirements and is not applied to clusters of commodity machines. Similarly (Áfra, 2012) presents a voxel-based paging system designed for interactive use, but it requires an expensive preprocessing step and displays visual artifacts at low LOD levels.

In (DeMarle et al., 2004), distributed shared memory is used to page in necessary data for rendering, but it relies on a complicated task scheduler to avoid flooding the network with large data blocks and it suffers from cache storms in a multithreaded environment. Efficient memory use is also the focus of (Moon et al., 2010), which obtains an order of magnitude speedup from reordering ray evaluation in a cache-oblivious way. This approach would complement our method very well.

The focus of (Reinhard et al., 1999), was development of a hybrid work scheduler which would improve performance with more effective hardware utilization, but it had problems with high memory overhead. Earlier this year, (Navrátil et al., 2012) presented an improved approach which uses a dynamic scheduler to move work from an image plane decomposition to a domain decomposition as rays begin to diverge.

A similar approach to ours was presented in (Badouel et al., 1994), but it failed to address the issue of shader execution within their asynchronous cluster design. Another similar approach is the Kilauea renderer in (Kato and Saito, 2002), but its pipeline is very latency sensitive and network communication is heavy due to rays being duplicated across many workers.

Recent research in strict out-of-core methods has focused on techniques for using main memory as an efficient cache. In (Kontkanen et al., 2011), they present a technique for dealing with huge point clouds used in point-based global illumination and demonstrate impressive cache hit rates of 95% and higher. Prior to that, (Pantaleoni et al., 2010) generated directional occlusion data using ray tracing, which was compressed into spherical harmonics for evaluation at render time. Ray tracing was not used for primary visibility. Like FlexRender, they also used hierarchical BVHs, but for the purpose of chunking scene data into

units of work that could be loaded into main memory quickly.

Using GPGPU techniques, (Garanzha et al., 2011), presented a method for ray tracing large scenes that are out-of-core on the GPU. Parts of their architecture are similar to FlexRender on a single-device scale, specifically their use of hierarchical BVHs and ray queues to handle rays cast from shaders. However, the global ray queue is fairly memory intensive, potentially storing up to 32 million rays.

Leveraging MapReduce (Dean and Ghemawat, 2004), an implementation of a ray tracer was presented by (Northam and Smits, 2011), but sending large amounts of scene data to workers significantly slowed down processing. Their solution was to break the scene into small chunks and resolve the intersection tests in the reduce step. Unfortunately, this does a lot of unnecessary work, because many non-winning intersections are computed that would have been pruned in a typical BVH traversal.

4 FlexRender ARCHITECTURE

In general, rendering with FlexRender proceeds in the following way:

1. Read in the scene data and define the maximum bounding extents of the entire scene. As data is read in, it is distributed to the workers using the Morton coding.
2. Once the scene is distributed, workers build BVHs in parallel for their respective local region of the scene. When complete, they send their maximum bounding extents to the renderer.
3. The renderer constructs a top-level BVH from each of the workers' bounds and sends this top-level BVH to all the workers.
4. Workers create image buffers. All shading computed on a worker is written to its own buffer.
5. Workers cast primary rays from the camera and test for intersections.
 - During intersection testing, rays may be forwarded over the network to another worker if they need to test geometry within the bounding extents of that worker.
 - Once the nearest intersection is found, illumination ray messages are created and sent to workers that have lights. These workers send light rays back towards the point of intersection to test for occlusion.
 - If the light rays reach the original intersection, the point is illuminated and the worker computes shading.
6. Once all rays have been accounted for, workers send their image buffers back to the renderer, which composites them together into a final image.

In the next few sections, we will examine each part of this process in greater detail.

4.1 Workers and the Renderer

There are two potential roles a machine can play during the rendering process.

Worker. These machines receive a region of the scene and act as ray processors, finding intersections computing shading. They produce an image that is a component of the final render. There may be an arbitrary number of workers participating.

Renderer. This machine distributes scene data to the workers. Once rendering begins it monitors the status of the workers and halts any potential runaway situations (see Section 4.4.3). When the renderer decides the process is complete, it requests the image components from each worker and merges them into the final image. There is only a single renderer in any given cluster.

The network architecture is client/server connected in a star topology. Each worker exposes a server which processes messages and holds client connections open to every other worker for passing messages around the cluster. The renderer also holds a client connection to every worker for sending configuration data, preparing the cluster for rendering (described in Section 4.3), and monitoring render progress (described in Section 4.5).

The current implementation does not include any provisions for fault tolerance. However, there is no architectural restriction preventing such measures. For topics involving the design of robust and resilient clusters, we refer the reader to the distributed systems literature.

The graphics machinery is fairly straightforward. A *scene* consists of a collection of *meshes*, which are stored as indexed face sets of vertices and faces. Each mesh is assigned a *material*, which consists of a *shader* and potentially a set of bindings from *textures* to names in the shader. A *shader* is a small program that computes the lighting on the surface at a particular point.

4.2 Fat Rays

The core message type in FlexRender is the *fat ray*. They are so named because they carry additional state information along with their geometric definition of an origin and a direction. Their counterparts, *slim rays*, consist of only the geometric components.

Specifically, a fat ray contains the following data, which is detailed in the subsequent sections:

- The **type of ray** this is.
- The **source pixel** that this ray contributes to.
- The **bounce count**, or number of times this ray has reflected off a surface (to prevent infinite loops).
- The **origin** and **direction** of the ray.
- The ray's **transmittance**, (related to the amount of its final pixel contribution).
- The **emission** from a light source carried along the ray, if any.
- The **target intersection point** of the ray, if any.
- The **traversal state** of the top-level BVH.
- The **hit record**, which contains the worker, mesh, and t value of the nearest intersection.
- The **current worker** this ray should be forwarded to over the network.
- The **number of workers touched** by the ray. (Not used for rendering, only analysis.)
- A **next pointer** for locally queuing rays. (Obviously invalid over the network.)

In total, the size of a fat ray is 128 bytes.

4.3 Render Preparation

To begin rendering FlexRender ensures that all the workers agree on basic rendering parameters, such as the minimum and maximum extents of the scene, which is used for driving Morton coding discretization along each axis. Once this data has been synchronized with all workers, each worker establishes client connections with every other worker that remain open for the duration of the render.

The renderer then divides up the 63-bit Morton code address space evenly by the number of workers participating and assigns ranges of the address space (which translate into regions of 3D space) to each worker. At this point the renderer begins reading in scene data and takes the following actions with each mesh:

1. Compute the centroid of the mesh by averaging its vertices.

2. Compute the Morton code of the mesh centroid. The range this falls in determines which worker the mesh will be sent to.
3. Ensure that any asset dependencies (such as materials, shaders, and textures) for this mesh are present on the designated worker.
4. Send the mesh data to the designated worker.
5. Delete the mesh data from renderer memory.

Although the current implementation reads scene data in at the renderer and distributes it over the network, there is no inherent reason why it needs to do so. For example, if all workers have access to shared network storage, the renderer could simply instruct each worker to load a particular mesh itself, reducing load time.

4.3.1 Parallel Construction of Bounding Volume Hierarchies

Next, workers construct a BVH for each mesh they have for accelerating spatial queries against the meshes. While building each BVH, the worker tracks bounding extents of each mesh. Workers then build a root BVH for the entire region owned by the worker with the mesh extents as its leaf nodes. When testing for intersections locally, a worker first tests against this root BVH to determine candidate meshes, then traverses each mesh's individual BVH to compute absolute intersections. After construction of this root BVH, the root node's bounding extents describe the spatial extent of all geometry owned by the worker.

Once construction of all local BVHs is complete, workers send their root bounding extents to the renderer. The renderer then constructs a final top-level BVH with worker extents as its leaf nodes. This top-level BVH is then distributed to all workers. This is a quick and lightweight process, since the number of nodes is only $2n - 1$, where n is the number of workers. This top-level BVH guides where rays are sent over the network in Section 4.4.4.

4.4 Ray Processing

Workers are essentially multithreaded ray processors. Their general work consists of processing rays by testing for intersection, potentially forwarding rays to another worker, or computing shading values if a ray terminates.

To manage these various tasks when all the geometry and lights may not be local to the worker, there are three different types of rays:

- **Intersection rays** are very much like traditional rays, which identify points in space that require shading.
- **Illumination ray messages** are copies of intersection rays that have terminated. They are sent to workers who have emissive geometry and assist in the computation of shading.
- **Light rays** are Monte Carlo samples that contribute direct illumination to a point being shaded.

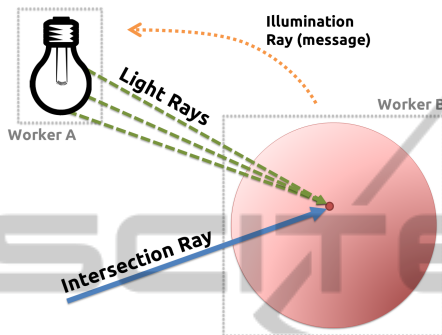


Figure 3: The three different ray types and their interactions.

The typical lifetime of these various rays is as follows:

1. An intersection ray is cast into the scene.
2. When that intersection ray terminates at a point in space, it dies and spawns an illumination ray message sent to each worker with emissive geometry.
3. When those illumination ray messages are delivered, they die and spawn light rays cast toward the original intersection.
4. If they terminate at the original intersection, the worker computes shading for it. When those light rays terminate, they die.

A single intersection ray can spawn many additional rays and light rays are the most likely to terminate without generating additional rays. These are key factors for deciding ray processing order for the cluster.

4.4.1 Illumination

In FlexRenderer there is no special “light” type, only meshes that are emissive, which is a property set by the assigned material. Emissive meshes are known to inject light into the scene through their shader. During scene loading, the renderer maintains a list of workers that have been sent at least one emissive mesh and sends the list to all workers before rendering begins.

Once intersection testing has identified a point needing shading, FlexRender must determine the visibility of light sources from that point. In a traditional

ray tracer, shadow rays are cast from the point of intersection to sample points on the surface of the light to determine visibility. However, from the perspective of the worker computing shading, it has no idea where the lights in the scene are, or if there is any geometry occluding the light, it just knows which workers have emissive meshes.

To solve this problem, illumination ray messages are used to request that emissive meshes instead test for visibility from their perspective. In this way, FlexRender traces an equivalent of shadow rays but in the opposite direction, which we call *light rays*. Instead of originating at the intersection point and traveling in the direction of the light, they originate at the light and travel in the direction of the intersection point. Area lights are supported through Monte Carlo integration by creating multiple light rays with origins sampled across the surface of the light.

If a light ray returns to the original intersection point after being traced through the cluster, which can be determined via the information carried forward in the *fat rays*, the renderer knows its path from the light was unoccluded. The advantage of this method is that it leverages the same method for tracing rays through a distributed BVH that used for testing ray intersections.

In summary, illuminating an intersection is done as follows:

1. On the worker where an intersection was found, copy the ray data into an illumination ray message with the target set to the point of intersection.
2. Send the illumination ray message to all emissive workers.
3. When a worker receives an illumination ray message, generate sample points across the surface of all emissive meshes. Set these sample points as the origins for new light rays.
4. Set the directions of all the light rays such that they are oriented in the direction of the target.
5. Push each light ray into the ray queue and let the cluster process them as usual.

4.4.2 Ray Queues

To manage the various types and numerous rays present in the system, each worker has a ray queue, with typical push and pop operations. Internally, this is implemented as three separate queues, where rays are separated by type. It also contains information about the scene camera, for generating new primary rays. When a new ray arrives at a worker, it is immediately pushed into the queue according to its type (intersection, illumination, or light).

When the worker pops a ray from the queue, rays are pulled from the internal queues in the following order:

1. The **light queue**, since these are least likely to generate new rays.
2. If the light queue is empty, the worker pops from the **illumination queue**, since these will generate a limited number of new rays.
3. If the illumination queue is empty, the worker pops from the **intersection queue**, since these can generate the most new rays.
4. If all of the internal queues are empty, the worker uses the camera to cast a new primary ray into the scene

Processing rays as a priority queue is essential for managing the exponential explosion of work that can occur if too many primary rays enter the system at once. It also helps reduce memory required for queuing because new work is not generated until the worker has nothing else to work on.

4.4.3 Primary Ray Casting

To give the cluster the ability to regulate itself, each worker in the cluster is responsible for casting a portion of the primary rays in the scene. Consider the case where a worker has not received any work recently from other workers in the cluster for whatever reason. By giving the worker control over primary ray casting for a portion of the scene, we enable workers to generate work when they have nothing to do.

However, in the case where a worker contains mostly background geometry, it will infrequently receive work from others because its size in screen space is small, yet it is in charge of casting primary rays for a larger slice of the image. In this case the worker may go on an unfettered spree of primary ray casting, generating lots of work for others and little for itself. To prevent this “runaway” case from overburdening the ray queues, workers report statistics about their progress to the renderer occasionally (10 times per second in our implementation). If a worker is getting significantly further ahead of the others in primary ray casting, the renderer temporarily disables primary ray casting on that worker.

This is not ideal, since lightly loaded workers will wait idle until they receive work to do, but it is simple to implement and works remarkably well in practice for mitigating the ray explosion and associated memory required for message queuing. See (Reinhard et al., 1999) and (Navrátil et al., 2012) for more sophisticated approaches that use dynamic scheduling to increase performance.

4.4.4 Distributed BVH Traversal

Distributed traversal of the scene BVH happens at two levels. Recall that the top level BVH contains bounding boxes for each worker and is present on all workers. Below that, each worker contains a BVH consisting of only the mesh data present on that worker.

When a ray is generated, traversal begins at the root of the top level tree and proceeds as described by (Hapala et al., 2011). When a leaf node intersection occurs closer to the camera than the current closest intersection, the traversal state is packed into the ray and the ray is forwarded to the candidate worker. The packed traversal state includes the index of the current top-level node and the state of the traversal automaton (*from the parent, from the sibling, or from the child*). The logic for top-level traversal is shown in Algorithm 1.

Algorithm 1: Top-level BVH traversal.

```

while current node != root do
  if ray intersects leaf node then
    if leaf node t < ray t then
      pack traversal state into ray;
      send ray to leaf node worker;
    end
  end
end
end

```

When a ray is received over the network and unpacked at the next worker, the traversal state is examined. If the traversal state points to the root of the top-level tree, the scene traversal has completed and the worker can shade the intersection if it was the worker on which that intersection occurred. Otherwise, the ray must be forwarded to the worker who won, since that worker has the shading assets.

If the traversal state is not at the root, the worker tests the ray against its local mesh BVH to find the closest intersection on this worker. If the result of that test is closer to the camera than the current closest intersection, the worker updates the hit record of the ray and resumes traversal of the top-level BVH by reinstating the traversal state packed into the ray and continuing where it left off. This logic is shown in Algorithm 2.

In the best case, a ray is generated on, intersects only with, and is shaded on a single worker. These rays never need to touch the network. In the worse case, the ray potentially intersects with all nodes, so it must touch every node in the tree.

In addition, there are two interesting corner cases to consider.

Algorithm 2: Worker-level BVH traversal.

```

if ray traversal state == root then
  if winning worker == this worker then
    | shade;
  else
    | send ray to winning worker;
  end
else
  test for intersections against worker BVH;
  if worker  $t <$  ray  $t$  then
    | write hit record into ray;
  end
  resume top-level traversal;
end

```

- If the ray is generated on a node that it does not intersect until later in the traversal, it consumes one additional network hop at the very beginning of the traversal.
- If the ray completes its traversal on a worker different from that which had the closest intersection, it consumes one additional network hop at the end of the traversal to put the ray on the correct worker for shading.

Thus, the worst case scenario actually touches $n + 2$ workers, where n is the number of workers in the cluster.

We discuss possible optimizations that may eliminate both of these corner cases in the Future Work Section. Additionally in Section 5, we show that in practice, the number of workers that each ray touches is less than or equal to the theoretical $O(\log n)$ performance of the binary tree for the majority of rays in the scene.

4.4.5 Shading

When a light ray arrives at a worker, it checks that its point of intersection is within some epsilon of the target. If it is, the worker considers the light sample visible, looks up the material, shader, and textures for the mesh, and runs the shader. The shader is responsible for writing its computed values into the worker's image buffer.

A shader may do any (or none) of the following:

- Sample textures.
- Compute light based on a shading model.
- Accumulate computed light into image buffers.
- Cast additional rays into the scene.

When new rays are cast into the scene from a shader, the results of that cast are not immediately

available. Instead, the cast pushes the new rays into the queue for processing and the traversal and shading systems ensure that the result of secondary and n -ary traced rays will be included in the final image. The source pixel of the new ray is inherited from its parent to ensure that it contributes to the correct pixel in the final image. In addition, the desired transmittance along the new ray is multiplied with the transmittance of the parent ray to ensure energy conservation is preserved.

4.5 Render Completion

In a traditional recursive ray tracer, determining when the render is complete is a simple task: When the last primary ray pops its final stack frame the render is over. In FlexRender, however, no one worker (or the renderer, for that matter) knows where the “last ray” is in the cluster. To determine when a render is complete, the workers report statistics about their activities to the renderer at regular intervals (in our current implementation, 10 times per second). We found the following four statistics to be useful for determining render completion:

Primary Ray Casting Progress. The amount of the worker's primary rays that have been cast into the scene.

Rays Produced. The number of rays created at the worker during this measurement interval. This includes new intersection rays cast from the camera or a shader, illumination ray messages created by terminating intersection rays, or light rays created by processing illumination ray messages.

Rays Killed. The number of rays finalized at the worker during this measurement interval. This includes intersection rays that terminated or did not hit anything, illumination ray messages that were destroyed after spawning light rays, or light rays who hit occluders or computed a shading value.

Rays Queued. The number of rays currently in this worker's ray queue.

If any worker has not finished casting its primary rays, we know for certain the render is not complete. Secondly, if no rays are produced, killed, or queued at any workers for some number of consecutive measurement intervals, it is reasonable to assume that the render has concluded. Our current implementation (reporting at 10 Hz) waits for 10 consecutive intervals of “uninteresting” activity on all workers before declaring the render complete. In practice, this achieves a reasonable balance between ending the render as quickly as possible and risking concluding it before all rays have been processed.

4.5.1 Image Synthesis

Once the render has been deemed “complete”, the renderer requests the image buffers from each worker. Because all rendering was computed by respecting linearity, computing a pixel in the final output image simply requires summing corresponding pixels in the worker buffers.

This process can yield some interesting intermediate images, as seen in Figure 4. Each worker’s buffer represents the light in the final image that interacts in some way with geometry present on that worker. For direct light, this shows up as shaded samples where geometry was present and dark areas where it was not. For other effects such as reflections and global illumination, we see the reflected light that interacted with the geometry present on the worker.

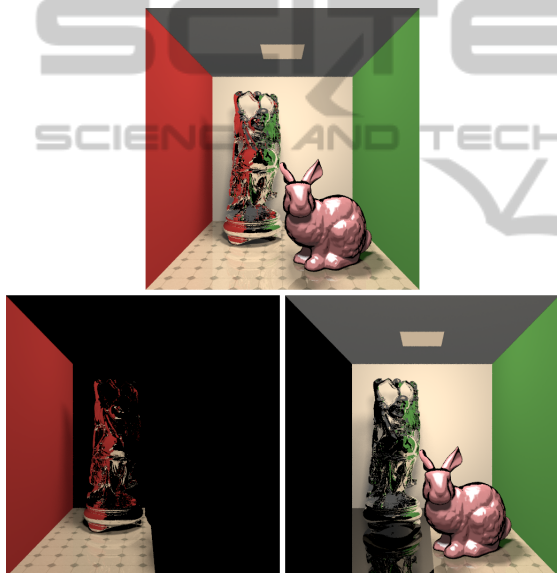


Figure 4: The bottom images show the geometry split between two workers. The composite image is on top. Note how the Buddha reflects the left side geometry in the left image and the right side geometry in the right image. The actual Buddha mesh data was distributed to the worker on the left.

5 RESULTS

For testing, we used 2-16 Dell T3500 workstations with dual-core Intel Xeon W3503 CPUs clocked at 2.4 GHz. Each workstation had 4 GB of system RAM, a 4 GB swap partition, and was running CentOS 6. FlexRender consists of around 14,000 lines of code, mostly C++. We leveraged several popular open source libraries, including *LuaJIT*, *libuv*, *MsgPack*, *GLM*, and *OpenEXR*. We used *pfstools* for tone

mapping our output images and *pdiff* for computing perceptual diffs.

5.1 Test Scene

Our test scene, “Toy Store”, has a geometric complexity of nearly 42 million triangles. The room geometry is relatively simple, but the toys on the shelves are unique (non-instanced) copies of the Stanford bunny, Buddha, and dragon meshes that have been remeshed from their highest quality reconstructions down to 14,249 faces, 49,968 faces, and 34,972 faces respectively. There are 30 toys per shelf and 42 shelves in the scene for a total of nearly 1,300 meshes. Approximately one quarter of the meshes are rendered using a mirrored shader, while the others used a standard Phong shader. The mirrored shader is what causes some black pixels in the image due to the scene not being completely enclosed. The scene consists of 1.09 GB of mesh data and 5 GB of BVH data once the acceleration structures are built.

We rendered a test image at a resolution of 1024x768 with no subpixel antialiasing, 10 Monte Carlo samples per light (32 lights in the scene), and a recursion depth limit of 3 bounces. For discussing speedups initially, we will focus on the 8-worker case (8 workers in the image plane decomposition configuration vs. 8 workers in the FlexRender configuration), but we will discuss varying cluster sizes in Section 5.6.

5.2 Image Plane Decomposition vs. FlexRender

In the image plane decomposition case, we consider 8 workers by chopping up the image into several vertical slices, with a different machine responsible for each slice (see Figure 5). The slices are then reassembled to form the final output image.

We report the time for each machine to complete each phase of rendering (loading the scene, building the BVH, and rendering its slice of the image) in Table 1. The total duration of the render would take 10,061 seconds (the slowest time), because the last slice is needed before the final image can be assembled. We report average times for the image plane decomposition workers compared to FlexRender for each of the 3 rendering phases in Table 2 and show FlexRender’s speedup over the average case of 6.57 times faster. We also report the total render time (all three phases combined), using the slowest image plane decomposition worker (time to final image).

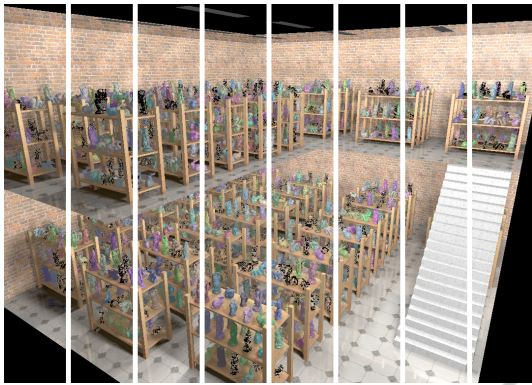


Figure 5: Slices of the Toy Store scene rendered with 8 machines using image plane decomposition (composite result image shown in Figure 6).

Table 1: Time for each phase of the IPD algorithm, for each of the 8 workers, in seconds. These include loading the scene, building the BVH, rendering the slice, and the total time of all three phases. Worker 4 was hit particularly hard with divergent secondary rays, and spent a large amount of time in I/O wait.

	Load	BVH	Render	Total
1	288	169	533	990
2	290	172	1119	1581
3	290	167	1491	1948
4	289	261	9511	10061
5	295	174	1792	2261
6	290	192	677	1159
7	287	167	1109	1561
8	294	171	303	768



Figure 6: Toy Store scene that is comprised of nearly 1,300 meshes and 42 million triangles.

5.3 Geometry Distribution

To ensure the entire scene stays in-core, FlexRender must distribute the geometry across the available

Table 2: Time (in seconds) for each phase of rendering with FlexRender versus the IPD configuration.

	IPD	FlexRender	Speedup
Loading	290.4 (avg)	326	0.89x
Build BVH	183.6 (avg)	20	9.18x
Rendering	2066.9 (avg)	1186	1.74x
Total	10061 (slowest)	1532	6.57x

Table 3: Percentage of rays that were processed by the given number of workers.

# of Workers	1	2	3	4
% of Rays	15.8%	25.6%	21.8%	18.8%
# of Workers	5	6	7	8+
% of Rays	8.9%	7.4%	1.5%	0.2%

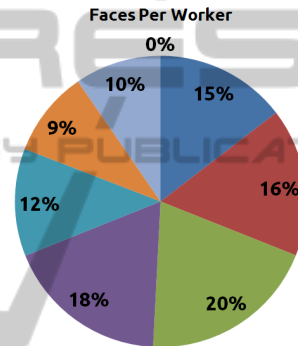


Figure 7: Percentage of total geometry that was distributed to each worker. Other than the worker with little geometry (top corner with only a fill light), the size of geometry per worker varied from 9% (106 MB of geometry and 488 MB of BVH data) to 20% (221 MB of geometry 1007 MB of BVH data) of the entire scene.

RAM in the cluster effectively. With the exception of one worker, the Morton coding and Z-order curve did a decent job of partitioning the scene data evenly. Figure 7 shows a breakdown of the geometry distribution. The one worker which did not contain very much geometry was in the top corner of the Toy Store closest to the camera. This octant of the scene only contained a fill light facing the rest of the geometry.

5.4 Network Hops

The intent of the top-level BVH is to reduce network cost by only sending rays across the network when they venture into that worker's region of space. Since a BVH exhibits $O(\log n)$ traversal, we expect that with 8 workers rays would be processed by 3 workers in the average case.

Table 3 shows that 63.2% of rays are handled by 3 workers or less, and nearly 16% never even re-

quire the network. (They are generated on, intersect with, and are shaded on a single worker.) In addition, 36.8% of rays must touch more than the expected 3 workers. However, including hops for the corner cases mentioned in Section 4.4.4, 82% of rays are at or below $O((\log n) + 1)$ and 90.9% of rays are at or below $O((\log n) + 2)$.

5.5 Ray Queue Sizes

Keeping the ray queue size small is critical to the long term health of the render. If rays begin queuing up faster than the cluster can process them, eventually the cluster will begin swapping when accessing rays, which violates our fundamental performance goal of staying in-core.

Because of this, we logged ray queue sizes on each worker over time while rendering Toy Store on a cluster of 16 workers. Figure 8 shows the queue sizes over time with workers represented as different colors. Table 4 breaks down the average queue size, as well as the maximum size over the course of the entire render and the storage demands of the maximum size, both in terms of raw storage space and a fraction of the system RAM.

Most workers sit comfortably below 1% of their RAM being used for queued rays, while the busiest worker used just over 1%. This demonstrates that our work throttling mechanisms, while simple, are keeping the cluster from generating more work than it can handle.

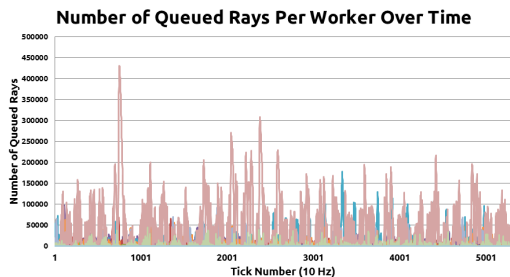


Figure 8: Number of rays queued on each worker over time. Different colors correspond to different workers.

5.6 Cluster Size

To evaluate the scalability of the FlexRender architecture, we ran Toy Store renders with cluster sizes of 4 workers, 8 workers, and 16 workers. For comparison, we ran the same renders in the image plane decomposition configuration also of 4, 8, and 16 workers.

Table 5 shows a continual and impressive improvement in the BVH construction time as the number of workers increases. This is thanks to the huge

Table 4: Size of ray queues when rendering Toy Store with a 16-worker FlexRender cluster.

	Avg Queued	Max Queued	Max Storage	Memory Use
1	107	12221	1.49 MB	0.04%
2	506	29796	3.64 MB	0.09%
3	969	34970	4.27 MB	0.10%
4	3116	57597	7.03 MB	0.17%
5	1687	36981	4.51 MB	0.11%
6	1430	44053	5.38 MB	0.13%
7	4070	80899	9.88 MB	0.24%
8	2000	16861	2.06 MB	0.05%
9	3767	97429	11.89 MB	0.29%
10	7921	178191	21.75 MB	0.53%
11	4477	69702	8.51 MB	0.21%
12	4943	92043	11.24 MB	0.27%
13	51164	430736	52.58 MB	1.28%
14	2193	45428	5.55 MB	0.14%
15	0	0	0 MB	0.00%
16	18	1374	0.17 MB	0.01%

Table 5: Comparison of cluster sizes with both image plane decomposition (IPD) and the FlexRender configuration (Flex). Times are in seconds.

# of Workers	4	8	16
IPD BVH Build	203	184	171
Flex. BVH Build	39	20	10
Speedup	5.21x	9.20x	17.1x
IPD Render	14833	10061	7702
Flex. Render	1742	1532	970
Speedup	8.51x	6.57x	7.94x
IPD Total	14536	9800	7413
Flex. Total	1405	1206	540
Speedup	10.35x	8.13x	13.73x

parallelization speedup from partitioning the scene geometry with Morton coding and building each subtree in parallel.

We also see render time improvements of roughly an order of magnitude, depending on how FlexRender chooses to distribute the geometry based on the number of workers available. It is likely that this performance advantage will slowly erode at much larger cluster sizes (due to increasing network communication costs), but for small to medium cluster sizes we see approximately linear growth.

5.7 Example Renders

Figure 6 shows the final Toy Store scene render, with nearly 42 million triangles and 1,300 meshes.

Figure 1 shows a scene with even higher resolu-

tion meshes, bringing the geometric complexity up to 87 million triangles, rendered on a cluster of 4 machines.

Figure 9 shows a monochromatic Cornell Box rendered by two workers. The final composite is on the left, while the individual image buffers are stacked on the right. With only direct lighting and no reflections, this clearly shows which geometry was assigned to each worker.

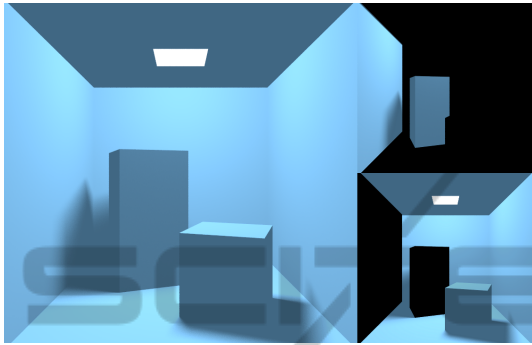


Figure 9: A monochromatic Cornell Box, showing the distribution of geometry between two workers.

Figure 10 demonstrates FlexRender’s Lua-based shader system. The bunny mesh is toon shaded, while the Buddha mesh has a perfect mirror finish. Reflection rays for the mirrored Buddha and floor are cast directly from the shaders.

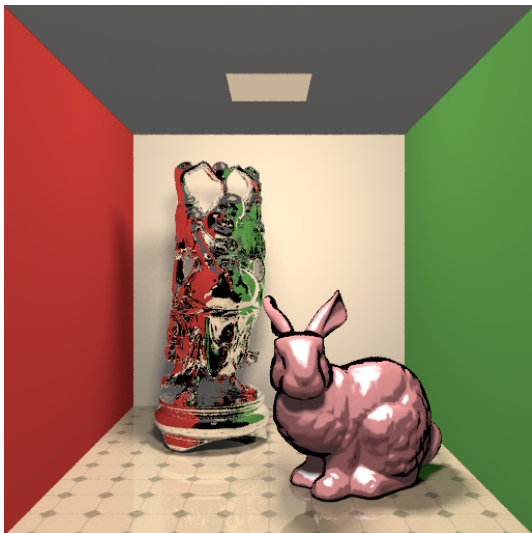


Figure 10: A Cornell Box with a toon shaded bunny and mirrored Buddha.

5.8 Summary

With these results, we have demonstrated that FlexRender meets our claimed contributions in the

following ways.

- Rays carry enough state to never require replies thanks to the feed-forward messaging design.
- This design allows the implementation of a shader system that requires no suspension of shader execution state as rays are moved between workers.
- FlexRender can correctly and efficiently traverse the scene when workers only contain spatially local BVHs, linked by a top-level BVH.
- The system keeps itself regulated and reduces memory usage by throttling new work generation and processing rays in an intelligent order.
- FlexRender shows consistent speedups over image plane decomposition, which suffers greatly from swapping to disk frequently during the rendering process.

5.9 Future Work

FlexRender could benefit from specialized tuning to scheduling and spatial distribution. Specifically, adding dynamic task scheduling as described in (Navrátil et al., 2012) could dramatically improve performance, and adopting a more sophisticated spatial distribution method as described in (Badouel et al., 1994) could also help with workload distribution.

The cache-oblivious ray reordering technique presented in (Moon et al., 2010) would complement our work quite nicely, and could offer another order of magnitude improvement in performance. Explorations with multiresolution geometry or coupling FlexRender with existing out-of-core methods would also dramatically increase the complexity of scenes FlexRender can handle efficiently.

With respect to our existing implementation, some network hops could be avoided when the ray finishes traversing the top-level BVH but ends up on a worker that is not the point of intersection. Because the worker has no shading assets for the terminating geometry, it must pass the ray back to the “winning” worker for shading. By distributing all of the shading assets (shaders, textures, and materials) to all workers, any worker would be capable of computing shading regardless of whether it was responsible for the terminating geometry.

Memory optimizations, such as object pooling, could exploit the transient nature of many fixed-size fat rays to reduce allocation overhead and heap fragmentation. In addition, the linear BVH node structures were intentionally padded to 64-bytes to match the cache line size on current CPUs. However without an aligned STL allocator for the vector that stores this array of nodes, cache alignment is not guaranteed.

Additionally, greater code optimization (e.g. use of SIMD instructions) could also improve performance.

Finally, one of FlexRender's strengths is that it decouples the ray tracing computations from shading with a feed-forward design that requires no replies. Because messages are both asynchronous and never return, this opens up the possibility for batching computation to specialized hardware coprocessors, such as GPUs or the upcoming Intel MIC cards.

REFERENCES

- Áfra, A. (2012). Interactive ray tracing of large models using voxel hierarchies. *Computer Graphics Forum*, 31(1):75–88.
- Badouel, D., Bouatouch, K., and Priol, T. (1994). Distributing data and control for ray tracing in parallel. *Computer Graphics and Applications, IEEE*, 14(4):69–77.
- Cignoni, P., Montani, C., Scopigno, R., and Rocchini, C. (1998). A general method for preserving attribute values on simplified meshes. In *Proceedings of the conference on Visualization '98, VIS '98*, pages 59–66, Los Alamitos, CA, USA. IEEE Computer Society Press.
- Clark, J. H. (1976). Hierarchical geometric models for visible-surface algorithms. In *Proceedings of the 3rd annual conference on Computer graphics and interactive techniques, SIGGRAPH '76*, pages 267–267, New York, NY, USA. ACM.
- Cohen, J., Olano, M., and Manocha, D. (1998). Appearance-preserving simplification. In *Proceedings of the 25th annual conference on Computer graphics and interactive techniques, SIGGRAPH '98*, pages 115–122, New York, NY, USA. ACM.
- Dean, J. and Ghemawat, S. (2004). Mapreduce: simplified data processing on large clusters. In *Proceedings of the 6th conference on Symposium on Operating Systems Design & Implementation - Volume 6, OSDI'04*, pages 10–10, Berkeley, CA, USA. USENIX Association.
- DeMarle, D. E., Gribble, C. P., and Parker, S. G. (2004). Memory-savvy distributed interactive ray tracing. In *Proceedings of the 5th Eurographics conference on Parallel Graphics and Visualization, EG PGV'04*, pages 93–100, Aire-la-Ville, Switzerland, Switzerland. Eurographics Association.
- Djeu, P., Hunt, W., Wang, R., Elhassan, I., Stoll, G., and Mark, W. R. (2011). Razor: An architecture for dynamic multiresolution ray tracing. *ACM Trans. Graph.*, 30(5):115:1–115:26.
- Garanzha, K., Bely, A., Premoze, S., and Galaktionov, V. (2011). Out-of-core gpu ray tracing of complex scenes. In *ACM SIGGRAPH 2011 Talks, SIGGRAPH '11*, pages 21:1–21:1, New York, NY, USA. ACM.
- Hapala, M., Davidovic, T., Wald, I., Havran, V., and Slusallek, P. (2011). Efficient stack-less bvh traversal for ray tracing. In *27th Spring Conference on Computer Graphics, SCCG '11*.
- Kato, T. and Saito, J. (2002). "kilauea": parallel global illumination renderer. In *Proceedings of the Fourth Eurographics Workshop on Parallel Graphics and Visualization, EGPGV '02*, pages 7–16, Aire-la-Ville, Switzerland, Switzerland. Eurographics Association.
- Kontkanen, J., Tabellion, E., and Overbeck, R. S. (2011). Coherent out-of-core point-based global illumination. In *Eurographics Symposium on Rendering*.
- Krishnamurthy, V. and Levoy, M. (1996). Fitting smooth surfaces to dense polygon meshes. In *Proceedings of the 23rd annual conference on Computer graphics and interactive techniques, SIGGRAPH '96*, pages 313–324, New York, NY, USA. ACM.
- Moon, B., Byun, Y., Kim, T.-J., Claudio, P., Kim, H.-S., Ban, Y.-J., Nam, S. W., and Yoon, S.-E. (2010). Cache-oblivious ray reordering. *ACM Trans. Graph.*, 29(3):28:1–28:10.
- Navrátil, P. A., Fussell, D. S., Lin, C., and Childs, H. (2012). Dynamic scheduling for large-scale distributed-memory ray tracing. In *Proceedings of Eurographics Symposium on Parallel Graphics and Visualization*, pages 61–70.
- Northam, L. and Smits, R. (2011). Hord: Hadoop online ray tracing with mapreduce. In *ACM SIGGRAPH 2011 Posters, SIGGRAPH '11*, pages 22:1–22:1, New York, NY, USA. ACM.
- Pantaleoni, J., Fascione, L., Hill, M., and Aila, T. (2010). Pantaray: fast ray-traced occlusion caching of massive scenes. In *ACM SIGGRAPH 2010 papers, SIGGRAPH '10*, pages 37:1–37:10, New York, NY, USA. ACM.
- Reinhard, E., Chalmers, A., and Jansen, F. W. (1999). Hybrid scheduling for parallel rendering using coherent ray tasks. In *Proceedings Parallel Visualization and Graphics Symposium*, pages 21–28.